

Addressing Attribute Leakages in Diffusion-based Image Editing without Training

Sunung Mun^{1*} Jinhwan Nam^{1*} Sunghyun Cho^{1,2} Jungseul Ok^{1,2†}

Graduate School of AI, POSTECH¹, Dept. of CSE, POSTECH²
{mtablo, njh18, s.cho, jungseul}@postech.ac.kr

Abstract

Diffusion models have become a cornerstone in image editing, offering flexibility with language prompts and source images. However, a key challenge is attribute leakage, where unintended modifications occur in non-target regions or within target regions due to attribute interference. Existing methods often suffer from leakage due to naive text embeddings and inadequate handling of End-of-Sequence (EOS) token embeddings. To address this, we propose ALE-Edit (Attribute-leakage-free editing), a novel framework to minimize attribute leakage with three components: (1) Object-Restricted Embeddings (ORE) to localize object-specific attributes in text embeddings, (2) Region-Guided Blending for Cross-Attention Masking (RGB-CAM) to align attention with target regions, and (3) Background Blending (BB) to preserve non-edited regions. Additionally, we introduce ALE-Bench, a benchmark for evaluating attribute leakage with new metrics for target-external and target-internal leakage. Experiments demonstrate that our framework significantly reduces attribute leakage while maintaining high editing quality, providing an efficient and tuning-free solution for multi-object image editing.

1. Introduction

Diffusion models for image generation [13, 35, 40] have emerged as a cornerstone technique for image editing [1, 3, 5, 7, 9, 14, 16, 19, 20, 27, 43, 46, 52], offering the ability to condition the image generation process on diverse inputs. Among these, editing an image based on a source image and a language prompt has gained significant attention due to the flexibility and intuitiveness of language-based controls.

Despite their potential, diffusion-based image editing faces key challenges, as these models are inherently de-

signed for generation rather than editing. Existing approaches often rely on fine-tuning diffusion models for specific editing tasks, which is computationally expensive [2, 28, 37, 42, 47]. To address this, recent efforts have introduced tuning-free methods, which bypass fine-tuning while aligning edits with user-specified prompts [1, 3, 5, 7, 9, 14, 16, 19, 20, 27, 43, 46, 52].

A critical issue in training-free image editing is *attribute leakage*, where unintended modifications occur outside the user-specified region. This issue can be categorized into: (1) target-external (TE) leakage: Unintended changes in non-target regions, such as background modifications, e.g., the first two rows of Figure 1; (2) target-internal (TI) leakage: Interferences between different target attributes, resulting in inconsistent or mixed attributes within target regions, e.g., the last two rows of Figure 1.

Despite extensive efforts, prior works [8, 48, 51] continue to struggle with severe attribute leakage. Specifically, our analysis identifies two overlooked origins of this issue: (1) the use of leakage-prone text embeddings, and (2) the persistent influence of End-of-Sequence (EOS) token embeddings. Due to the recurrent nature of the CLIP text encoder, embeddings for words later in the prompt inherently encode the semantic information of earlier attributes. This makes naive text embeddings particularly susceptible to attribute leakage, as they embed unintended relationships between attributes.

To mitigate this, some approaches [8] propose generating separate embeddings for each target object. While this helps reduce interference, these methods often combine the newly generated embeddings with the original prompt embeddings by averaging, which leaves room for attribute leakage to persist. Additionally, EOS token embeddings, commonly used for padding, encapsulate the global semantic information of the entire prompt. Despite their significant role in propagating unintended information, the contribution of EOS embeddings to attribute leakage has been largely overlooked in prior works.

As demonstrated in Figure 2, using the original EOS em-

*: Equal contribution; †: Correspondence to jungseul@postech.ac.kr
Project page: https://mtablo.github.io/ALE_Edit_page/

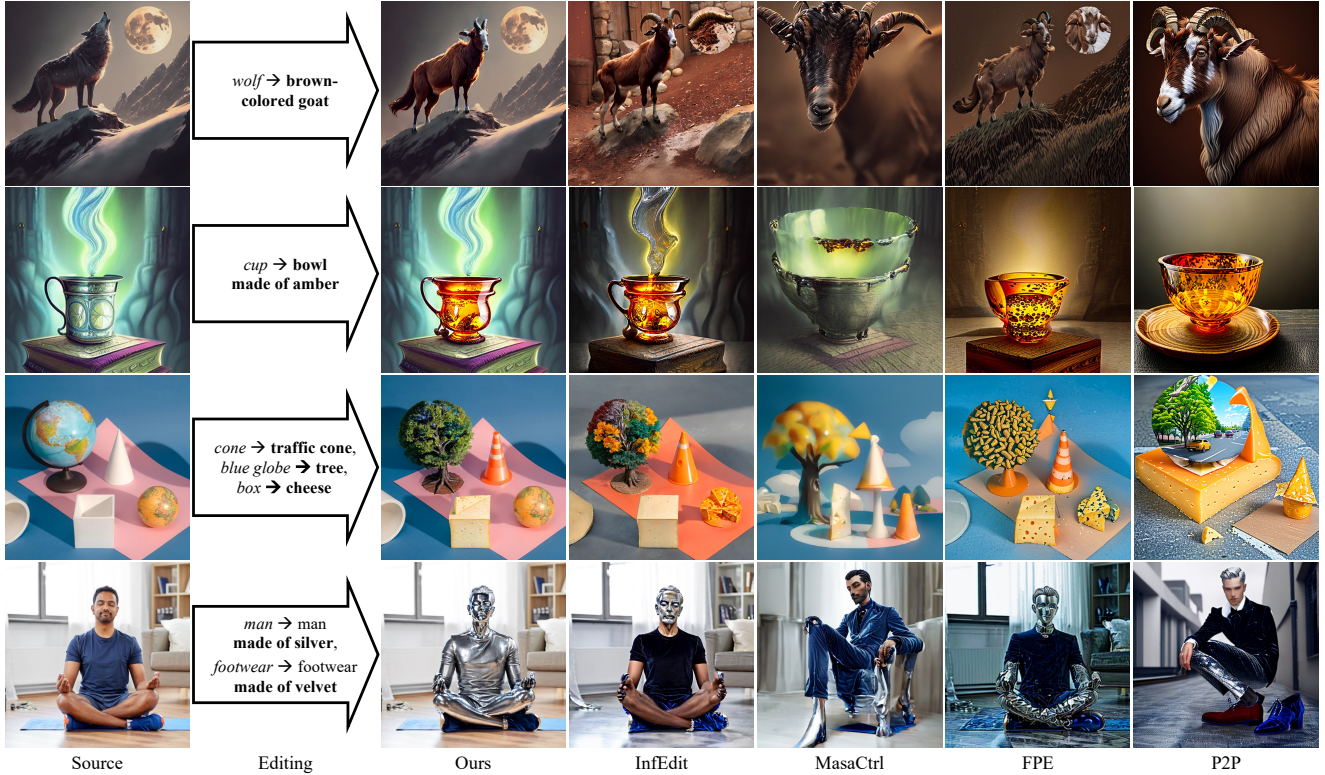


Figure 1. Comparison of tuning-free image editing methods. The left side of \rightarrow represents the *source object*, and the right side represents the **target object**. The first two rows demonstrates cases of target-external leakage, where other methods either modify unintended regions or fail to preserve the structural integrity of the source image. The last two rows highlights target-internal leakage, where interactions between target attributes result in inconsistent or undesired edits. Our method, ALE-Edit, achieves accurate and consistent edits, preserving structural details and preventing both target-external and target-internal leakage.



(a) Source image (b) Original EOS (c) EOS $\leftarrow \mathbf{0}$ (d) EOS $\leftarrow \text{""}$

Figure 2. Comparison of EOS embedding modification methods for editing “yellow paprika” to “**diamond**” and “red paprika” to “**moon**”. (b) Original EOS embeddings. (c) Replacing EOS embeddings with zero vectors. (d) Replacing EOS embeddings with EOS embeddings from an empty string “”.

beddings during editing can lead to attribute leakage, such as diamond-like structures appearing on the moon. While naive methods for modifying EOS embeddings—such as replacing them with zero vectors or embeddings derived from an empty string—can reduce attribute leakage, they significantly degrade editing quality, resulting in unrealistic or incomplete outputs. This highlights the critical role of properly constructed EOS embeddings in achieving both attribute-leakage-free and high-quality image editing.

Cross-attention layers further exacerbate this issue. Though several approaches attempt to modify attention mechanisms [4, 11, 14, 15, 17, 19, 21, 22, 25, 26, 29, 31,

38, 47, 51, 52] to constrain the regions of the image that each token can attend to, they often overlook the effect of EOS tokens and embeddings to address their complex interactions within cross-attention.

To tackle these challenges, we propose ALE-Edit (**A**tttribute-**L**eaKage-free **E**dit**I**ng), a novel framework to minimize attribute leakage by refining text embeddings and the cross-attention mechanism through three key components:

1. **Object-Restricted Embeddings (ORE)**: localizing object-specific attributes in text embeddings to restrict unintended interactions.
2. **Region-Guided Blending for Cross-Attention Masking (RGB-CAM)**: enhancing cross-attention using precise object and background masks to align attention with intended regions.
3. **Background Blending (BB)**: preserving non-edited regions by blending source and target latents based on background masks.

Furthermore, to comprehensively evaluate attribute leakage, we introduce a new benchmark, ALE-Bench. To enable robust evaluation, our benchmark includes a diverse set of editing scenarios, covering various types of edits across

multiple objects within an image. ALE-Bench addresses limitations in prior evaluations by incorporating diverse editing scenarios and introducing two novel metrics—TE leakage and TI leakage—for precise measurement of attribute leakage.

Extensive experiments demonstrate the efficacy of ALE-Edit, achieving superior results across multi-object editing scenarios as seen in Table 1. By addressing key limitations of existing methods, our approach provides a robust, training-free solution for image editing. The primary contributions of this work are as follows:

- We propose ALE-Edit, a training-free image editing framework that significantly mitigates attribute leakage, enabling user-friendly edits with minimal prompt requirements.
- We analyze and identify critical sources of attribute leakage in diffusion models, including naive text embeddings, EOS embeddings, and cross-attention layers.
- Our method minimizes attribute leakage through three novel components: Object-Restricted Embeddings (ORE), Region-Guided Blending for Cross-Attention Masking (RGB-CAM), and Background Blending (BB).
- We introduce ALE-Bench, a benchmark for evaluating attribute leakage in multi-object editing scenarios, providing a comprehensive and precise measurement of attribute leakage as well as editing performance.

2. Problem Formulation

2.1. Preliminaries

Diffusion model Diffusion models [13] are generative models that use a noise schedule to progressively corrupt data during training and reverse the process during sampling. The forward process is formulated as:

$$x_t = \sqrt{\alpha_t}x_0 + \sqrt{1 - \alpha_t}\epsilon, \epsilon \sim N(0, \mathbf{I}), \quad (1)$$

where x_0 is a clean sample following the data distribution, α_t a variance schedule, and x_t a noisy sample. Sampling is performed by the reverse process, formulated as:

$$x_{t-1} = \sqrt{\alpha_{t-1}}\bar{x}_0 + \sqrt{1 - \alpha_{t-1} - \sigma_t^2} \cdot \epsilon_\theta(x_t, t) + \sigma_t \epsilon_t, \quad (2)$$

where $\bar{x}_0 = \frac{x_t - \sqrt{1 - \alpha_t} \cdot \epsilon_\theta(x_t, t)}{\sqrt{\alpha_t}}$ is expected x_0 , ϵ_θ is a noise prediction model, and σ_t is a noise schedule. For text-conditioned diffusion models, the noise prediction model is defined as $\epsilon_\theta(x_t, t, y)$, where y denotes a text prompt.

Attention control Attention control is a technique for conditioning text-to-image diffusion models on images, even though these models are not explicitly trained to take images as inputs. Prompt-to-Prompt (P2P) [11] first demonstrated the utility of this method by manipulating cross-attention layers. Specifically, P2P injects

cross-attention mappings from the reconstruction of the source image into the generation process of the target image. Building on this idea, MasaCtrl [3] and Free-Prompt-Editing (FPE) [20] proposed using self-attention for attention control. Both methods involve injecting self-attention values from the source into the target. MasaCtrl modifies the target self-attention by combining it as $\{Q_{target}, K_{target}, V_{source}\}$, whereas FPE takes the approach of forming $\{Q_{source}, K_{source}, V_{target}\}$.

Inversion-free Image Editing Inversion-free image editing, introduced as Virtual Inversion in InfEdit [46], is a tuning-free approach for image editing. While several works [28, 42, 47] have aimed to reduce reconstruction errors, they typically incur significant computational costs, often taking several minutes per image. In contrast, Virtual Inversion achieves accurate reconstruction without parameter tuning by directly addressing the error. It subtracts the reconstruction error as follows: $\Delta\epsilon_t^{cons} = \epsilon_\theta(z_0^{src}, \epsilon, t) - \epsilon$, where $\Delta\epsilon_t^{cons}$ represents the expected error. This error is then used to refine the denoising process in the target branch. With this approach, only a few steps are needed to generate an edited image that maintains the quality of the original source image, offering both efficiency and high fidelity.

Limitations Injecting cross-attention values poses difficult challenges when handling prompts with substantially different structures, as the alignment between the source and target prompts becomes less intuitive. Another limitation is the reliance on user expertise; fully utilizing these methods often demands skilled users and involves extensive trial and error in crafting effective text prompts. Additionally, prior works have overlooked the critical role of EOS tokens in guiding text-to-image generation, underestimating their influence on the output quality and alignment.

2.2. Image Editing

Unlike image generation, image editing has a distinct goal: modifying specific regions of a given image while preserving all other areas. Formally, given a source image x^S , source prompt y^S , and target prompt y^T , the objective of image editing is to generate a new image x^T . This image x^T must satisfy two key constraints: (1) the region of x^S corresponding to y^S should be modified to match the description in y^T , and (2) all other regions of x^S should remain unchanged. Failure to satisfy either constraint results in an unsatisfactory x^T : an image that either fails to align with y^T or deviates from x^S by altering unrelated regions.

2.3. Attribute Leakage

A significant challenge in image editing is the issue of attribute leakage, which results from inherent limitations in

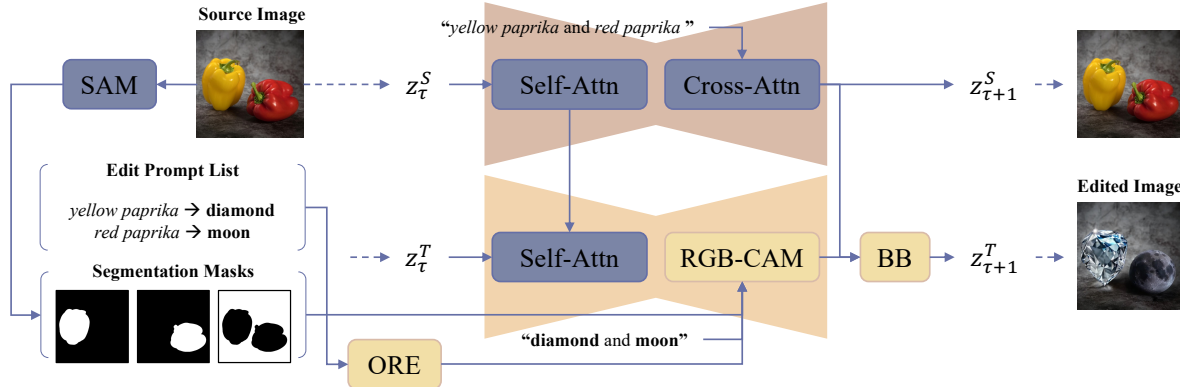


Figure 3. Overview of our proposed image editing method. The framework consists of two branches: the upper part (source branch) processes the source latent z_τ^S , and the lower part (target branch) processes the target latent z_τ^T at each timestep τ . The method comprises three key components: Object-Restricted Embeddings (ORE), Region-Guided Blending for Cross-Attention Masking (RGB-CAM), and Background Blending (BB). ORE generates attribute-leakage-free embeddings to minimize interference between unrelated objects. RGB-CAM leverages segmentation masks from Grounded-SAM to refine cross-attention activations, aligning attention to specific regions for each target object. BB integrates the source latent for background regions and the target latent for edited regions.

pre-trained diffusion models. Image editing frameworks often fail to precisely apply the specified attributes to target objects, resulting in unintended modifications.

For example, in the first row of Figure 1, where the task is to edit a “*wolf*” into a “**brown-colored goat**”, many methods exhibit target-external attribute leakage. These leakages manifest as unexpected changes to the surrounding environment, such as introducing additional **goats** or altering the **brown** background, which were not part of the editing prompt.

Similarly, in the last row of Figure 1, when editing a “*man*” into “man made of **silver**” and “*footwear*” into “footwear made of **velvet**”, other methods often suffer from both target-external and target-internal attribute leakage. Target-external leakage includes changes to unrelated regions, such as parts of the background adopting unintended attributes. Target-internal leakage occurs when attributes like “**velvet**” incorrectly extend to other target objects, compromising the consistency and precision of the edits.

These various forms of attribute leakage are challenging to detect using existing metrics, such as the CLIP similarity score between target prompts and edited images. To address this, we propose two new metrics in Section 4.1: target-external (TE) leakage and target-internal (TI) leakage, specifically designed to evaluate these distinct types of attribute leakage.

2.4. Limitations of Existing Methods

StructureDiffusion [8] extracts and encodes target object noun phrases (NPs) separately to create TI leakage-free embeddings. However, these embeddings are averaged with the base prompt embedding, which remains prone to attribute leakage. This averaging process and the oversight of EOS embeddings in the editing process allow attribute

leakage to persist.

RPG [48] indirectly addresses the EOS issue by rephrasing a single prompt into multiple subprompts, each describing an object. However, it relies on a base prompt to preserve spatial consistency, which introduces attribute leakage as base prompt attributes can unintentionally affect other regions. Additionally, processing subprompts independently leads to coherence issues if the base prompt is removed and requires separate denoising for each object, resulting in high computational costs.

SPDiffusion [51] proposed using masks to specify regions where certain objects should not be generated, whereas our method specifies regions where objects should be generated. While the approaches are similar in concept, SPDiffusion does not account for how text embeddings can influence cross-attention and contribute to attribute leakage, leaving this important issue unaddressed.

3. Proposed Method

We address the image editing task: generating a target image x^T from a source image x^S , guided by pairs of text prompts $[(y_{O_i^S}, y_{O_i^T})]$. Each pair specifies the edit of a source object into a target object, where $y_{O_i^S}$ describes the i -th object in the source image, and $y_{O_i^T}$ describes its corresponding target object. To minimize attribute leakage and enable precise edits, ALE-Edit address three major objectives:

1. Attribute-leakage-free text embeddings: addressing unintended attribute leakage caused by naive text embeddings through Object-Restricted Embeddings (ORE).
2. Attention alignment: aligning target object tokens to attend only to its designated regions through Region-Guided Blending Cross-Attention Masking (RGB-CAM).

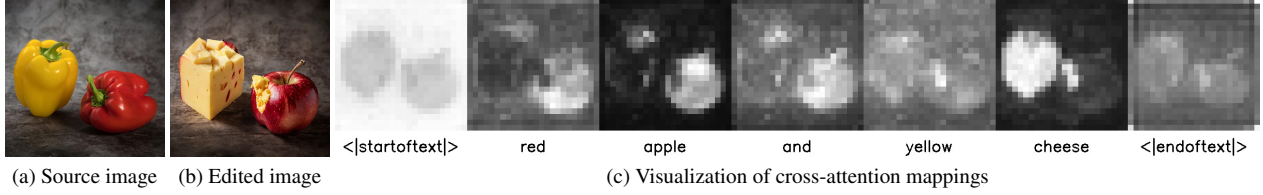


Figure 4. Example of severe target-internal leakage in the cross-attention layer causing misplacement of target objects. The task is to change “yellow paprika” into “red apple” and “red paprika” into “yellow cheese”. However, due to unintended attention mappings, the positions of the target objects are swapped. Cross-attention mappings in Figure 4c are averaged across all timesteps.

3. Background preservation: preserving non-edited regions of the image through Background Blending (BB).

By addressing these challenges step-by-step, our method ensures precise, consistent image editing while effectively mitigating both target-internal and target-external attribute leakage. Each of these methods is addressed in detail in Sections 3.1, 3.2, and 3.3, respectively.

3.1. Object-Restricted Embeddings

In the CLIP text encoder, every word in a prompt influences all subsequent words, leading to unintended links between unrelated attributes. This cumulative structure causes the EOS (End-of-Sequence) embedding to implicitly encode information about the entire text prompt. As a result, the EOS embedding can cause attribute leakage via cross-attention layers in diffusion models. To address this issue, we propose the Object-Restricted Embeddings (ORE) method, as described in Algorithm 1.

Our method takes as input paired text prompts in the form of $[(y_{O_1}^S, y_{O_1}^T), (y_{O_2}^S, y_{O_2}^T), \dots]$, where each pair specifies the edit of an object in the source image to its corresponding target object. Here, O_i represents i -th object, y_{O_i} denotes the text prompt describing O_i . From these pairs, we construct a base source prompt and a base target prompt by concatenating the source and target objects with “and”.

To generate object-restricted embeddings, we first encode the entire base prompt as a single sequence to obtain e_{base} . Then, each object-specific prompt $\{y_{O_i}\}$ is encoded individually to obtain $\{e_{O_i}\}$. The object embeddings $e_{O_i}[O_i]$ are then substituted into the corresponding positions of e_{base} , ensuring that the attributes of each object replace only their relevant parts in the base prompt embeddings. This substitution preserves the overall structure of the base prompt while isolating the attributes of individual objects.

To further mitigate attribute leakage caused by EOS embeddings, we modify the embeddings to focus exclusively on the target object. Specifically, for each target object, unrelated parts of e_{base} are set to zero, and the original EOS embeddings are replaced with the object-restricted embeddings. These modified embeddings are applied in the cross-attention layers to ensure they activate only in regions corresponding to their respective objects, enabling precise and attribute-leakage-free image editing.

Algorithm 1 Object-Restricted Embeddings

Input Object list $[y_{O_1}, y_{O_2}, \dots]$, a base prompt y_{base}
Output Object-restricted embeddings $[e'_{base}, e'_{O_1}, \dots]$

- 1: $e'_{base} \leftarrow \text{Encoder}_{text}(y_{base})$
- 2: $N \leftarrow \text{length}([y_{O_1}, y_{O_2}, \dots])$
- 3: **for** i in $\text{range}(N)$ **do**
- 4: $e_{O_i} \leftarrow \text{Encoder}_{text}(y_{O_i})$
- 5: $e'_{base}[O_i] \leftarrow e_{O_i}[O_i]$
- 6: $e'_{O_i} \leftarrow e'_{base}$
- 7: **for** j in $\text{range}(N)$ and $i \neq j$ **do**
- 8: $e'_{O_i}[O_j] \leftarrow \mathbf{0}$
- 9: **end for**
- 10: $e'_{O_i}[\text{EOS index}_i :] \leftarrow e_{O_i}[\text{EOS index}_i :]$
- 11: **end for**
- 12: **return** $[e'_{base}, e'_{O_1}, e'_{O_2}, \dots]$

3.2. Region-Guided Blending for Cross-Attention Masking

Even with ORE e'_{base} , constructed to minimize attribute leakage, unintended attention mappings can still occur in cross-attention layers. These layers sometimes activate irrelevant regions of the image, leading to target-internal leakage. For example, in Figure 4, the attention map for the token “apple” incorrectly activates the region corresponding to the “yellow cheese”, while the attention for “cheese” overlaps with the region of the “red paprika”. These misaligned activations demonstrate how cross-attention layers can propagate unintended attribute leakage even when using ORE.

To address this issue, we propose RGB-CAM (Region-Guided Blending for Cross-Attention Masking) in Algorithm 2, a method that explicitly defines the spatial regions each target object should attend to. This is achieved by utilizing segmentation masks $\{m_i\}$ that specify the areas in the image associated with each object. The masks $\{m_i\}$ are generated using Grounded-SAM [18, 23, 34]. Since masks generated by Grounded-SAM are often slightly smaller than the actual object regions, we apply a slight dilation to improve transitions along object boundaries.

In RGB-CAM, the cross-attention output for each object is calculated in a region-specific manner. First, for each ORE e'_{O_i} , we compute its corresponding cross-attention

value v_{O_i} . The cross-attention map M_{base} , derived from the query and key projections of latent and e_{base} , is multiplied with v_{O_i} to produce the cross-attention output A_{O_i} for each object. This output is then restricted to its designated regions using the corresponding segmentation mask m_i .

For the background and overlapping regions, we compute a base attention output A_{base} from v_{base} , derived from the e_{base} . The final cross-attention output A is constructed by combining A_{base} (for the background and overlapping regions) with the masked outputs A_{O_i} (for each object):

$$A = A_{base} \odot m_{back} + \sum_i (A_{O_i} \odot m_i). \quad (3)$$

By blending object-specific attention outputs with a base attention output for the background, RGB-CAM ensures that each token focuses exclusively on its assigned regions. This method effectively prevents attribute leakage, preserving the spatial consistency of the image and producing high-quality editing results.

Algorithm 2 RGB-CAM

Input Target latent z , base prompt y_{base} , ORE list $[e'_{base}, e'_{O_1}, e'_{O_2}, \dots]$, object masks $[m_1, m_2, \dots, m_{back}]$

Output Attribute-leakage-free cross-attention output A

```

1:  $q \leftarrow \text{proj}_Q(z)$ 
2:  $k \leftarrow \text{proj}_K(\text{Encoder}_{text}(y_{base}))$ 
3:  $v_{base} \leftarrow \text{proj}_V(e'_{base})$ 
4:  $m\_list \leftarrow \text{associate\_masks}(y_{base}, [m_1, m_2, \dots, m_{back}])$ 
5:  $M_{base} \leftarrow \text{get\_attention\_map}(q, k, m\_list)$ 
6:  $A_{base} \leftarrow M_{base} * v_{base}$ 
7:  $A \leftarrow A_{base}$ 
8:  $N \leftarrow \text{length}([e'_{O_1}, e'_{O_2}, \dots])$ 
9: for  $i$  in  $\text{range}(N)$  do
10:    $v_{O_i} \leftarrow \text{proj}_V(e'_{O_i})$ 
11:    $A_{O_i} \leftarrow M_{base} * v_{O_i}$ 
12:    $A \leftarrow A \odot (\mathbf{1} - m_i) + A_{O_i} \odot m_i$ 
13: end for
14: return  $A$ 

```

3.3. Background Blending

While ORE and RGB-CAM effectively ensure that target object attributes are generated in their intended regions, non-edited areas are processed using a succinct base prompt focused solely on the target objects. This lack of detailed guidance often results in significant target-external (TE) leakage, as the background is edited with no information about the original background. To address this, we propose a Background Blending (BB) method that leverages the source latent to preserve non-edited regions.

Local blending [11, 46] has been widely adopted for background preservation in image editing tasks. This approach involves generating masks of regions not to edit by

thresholding cross-attention maps. However, generating accurate masks using cross-attention maps is challenging because it is difficult to obtain precise masks, and setting an appropriate threshold often requires numerous trials and errors. Moreover, when editing multiple objects, determining suitable thresholds and text prompts becomes even more time-consuming and complex.

To overcome these challenges, we propose a Background Blending (BB) method that uses segmentation masks obtained from Grounded-SAM to preserve non-edited regions explicitly. Specifically, the masks of the source objects are used to generate a background mask m_{back} , which identifies the areas corresponding to non-edited regions in the image. At each denoising step τ , BB blends the source branch latent z^S for the background regions with the target branch latent z^T for the object regions to create a new latent $\tilde{z}_{\tau+1}$:

$$\tilde{z}_{\tau+1}^T = m_{back} \odot z_{\tau+1}^S + (1 - m_{back}) \odot z_{\tau+1}^T. \quad (4)$$

By using the source latent for non-edited regions, BB effectively preserves the non-edited regions while minimizing TE leakage.

4. Experiments

4.1. Benchmark Construction

While attribute leakage weakens the precision and reliability of image editing methods, existing benchmarks often overlook evaluating this issue. Furthermore, since most methods require detailed image descriptions as prompts to achieve good editing results, most benchmarks typically provide extensive source-target prompt pairs. For example, they may require “a wolf on a snowy mountainside on a full moon night” as the source prompt and “a dog on a snowy mountainside on a full moon night” as the target prompt. However, this does not reflect real-world scenarios where users prefer **succinct** instructions; in the above case, users may simply use “wolf” and “dog” as prompts.

To address these gaps, we introduce a novel benchmark ALE-Bench (Attribute Leakage Evaluation Benchmark) specifically designed to evaluate attribute leakage with succinct prompts. Our benchmark includes succinct editing prompts crafted to assess attribute leakage and proposes a new metric to effectively measure it. We randomly generated 300 edits templates by utilizing 20 source images and five types of edits, varying the number of objects edited from one to three. For each template, we created 10 random edits instances, resulting in total 3,000 image edits.

Image selection ALE-Bench comprises 20 images, evenly divided between natural and artificial images to cover diverse scenes. All images are sourced from free image repositories or PIE-bench [7] dataset. Each image contains at least three distinct objects to ensure sufficient

Method	TE Leakage	TI leakage	Structure Preservation	Editing Performance	Background Preservation			
	CS ↓	CS ↓	SD ↓	Edited ↑	PSNR ↑	LPIPS ↓	MSE ↓	SSIM ↑
P2P	21.48	17.19	0.1529	20.61	11.13	0.4493	0.0885	0.5583
MasaCtrl	20.12	16.62	0.0930	19.89	14.96	0.2946	0.0423	0.7329
FPE	21.06	17.28	0.1183	21.78	12.79	0.3912	0.0663	0.6020
InfEdit	19.58	16.59	0.0487	21.68	16.69	0.2049	0.0344	0.7700
Ours	16.03	15.28	0.0167	22.20	30.04	0.0361	0.0014	0.9228

Table 1. Comparison of attribute leakage and traditional metrics across editing methods on ALE-Bench. Our method demonstrates the lowest attribute leakage, highest structure preservation, and superior editing performance, indicating a more precise and controlled editing. CS represents CLIP Similarity, SD represents Structure Distance.

# of Editing Objects	TE Leakage	TI leakage	Structure Preservation	Editing Performance	Background Preservation			
	CS ↓	CS ↓	SD ↓	Edited ↑	PSNR ↑	LPIPS ↓	MSE ↓	SSIM ↑
1	16.21	NaN	0.00885	22.54	30.13	0.0394	0.00134	0.9046
2	15.97	15.31	0.01660	21.97	30.04	0.0362	0.00139	0.9223
3	15.91	15.26	0.02462	22.09	29.94	0.0328	0.00158	0.9414

Table 2. Performance of ALE-Edit on ALE-Bench based on the number of objects edited. Our method maintains low attribute leakage and strong background preservation even as the number of editing objects increases.

complexity for evaluating attribute leakage across multiple entities within a scene. Additionally, we generate source object masks to be used for metric computations by manually refining the result masks of Grounded-SAM.

Prompt construction We define five editing types: *color change*, *object change*, *material change*, *color and object change*, *object and material change* to simulate various real-world editing scenarios. In addition, we vary the number of object to be edited in each image from one to three. Finally, we utilized ChatGPT to generate the attribute lists of colors, new object, and materials for the source objects to be edited. By covering various editing cases, ALE-Bench can robustly evaluate the editing method’s ability to prevent attribute leakage.

Evaluation metric To quantify the performance of image editing models and specifically measure attribute leakage, we employ standard image quality metrics and introduce novel metrics tailored for this purpose. For assessing overall editing performance, we utilize structural distance [44], background preservation metrics [46], CLIP similarity. However, these metrics have limitations in capturing the degree of attribute leakage. To address this, we define two new metrics.

Target-Internal (TI) leakage assesses unintended cross-influence between edited targets when multiple objects are edited simultaneously. We compute the CLIP similarity between each edited object’s region and the prompts for the other targets, then take the mean of similarity scores across

all pairs as follows:

$$TI = \frac{1}{N(N-1)} \sum_{i \neq j} \text{CLIP}(I_e \odot m_j, y_i^T), \quad (5)$$

Lower TI values suggest that edits have been well isolated to the intended objects without affecting others.

Target-External (TE) leakage quantifies unintended alterations in the background (non-edited region) due to the editing. This metric is calculated by computing the CLIP similarity between the background region of the edited image and the target prompt, as follows:

$$TE = \frac{1}{N} \sum_{i=1}^N \text{CLIP}\left(I_e \odot \left(\mathbf{1} - \bigcup_{j=1}^N m_j\right), y_i^T\right), \quad (6)$$

where CLIP is the CLIP similarity score, N is the number of objects to be edited, I_e is the edited image, m_j is the j -th object mask, and y_i^T is the target prompt for i -th object. For multiple object edits, we calculate the mean CLIP similarity scores between the background and each target prompt. Lower TE values indicate minimal leakage, meaning the outside of targets remains unaffected by the edits intended for the targets.

4.2. Main Results

Our method, ALE-Edit, demonstrates superior performance in attribute leakage control and image editing quality compared to existing methods, as seen in Table 1. Specifically, our method achieves the lowest scores in both TE and TI

Editing Type	TE Leakage	TI leakage	Structure Preservation	Editing Performance	Background Preservation			
	CS ↓	CS ↓	SD ↓	Edited ↑	PSNR ↑	LPIPS ↓	MSE ↓	SSIM ↑
Color	17.66	15.93	0.00913	22.85	32.89	0.0294	0.00080	0.9293
Object	15.80	16.28	0.01986	21.81	29.07	0.0382	0.00166	0.9212
Material	17.09	15.71	0.01204	22.78	30.58	0.0344	0.00121	0.9235
Color+Object	15.15	14.00	0.02277	22.14	28.70	0.0399	0.00178	0.9204
Object+Material	14.47	14.49	0.01967	21.42	28.94	0.0387	0.00172	0.9195

Table 3. Performance of ALE-Edit on ALE-Bench across various editing types (color, object, material, and combinations). The results show consistent low attribute leakage and high editing performance.



Figure 5. Qualitative examples of ALE-Edit for each editing type in three objects editing. Color prompt: *tree* → **blue-colored** tree, *couch* → **purple-colored** couch, *floor* → **khaki-colored** floor. Object prompt: *tree* → **pine tree**, *couch* → **bench**, *floor* → **lawn**. Material prompt: *tree* → tree made of **diamond**, *couch* → couch made of **leather**, *floor* → floor made of **turquoise**. Color+Object prompt: *tree* → **yellow-colored Christmas tree**, *couch* → **khaki-colored desk**, *floor* → **yellow-colored tile**. Object+Material prompt: *tree* → **pine tree made of bamboo**, *couch* → **desk made of chrome**, *floor* → **tile made of jade**.



Figure 6. Qualitative examples for ablation over RGB-CAM and BB.

attribute leakage, indicating a more precise application of attributes only to the specified target regions. Table 2 shows that our method remains robust across different numbers of editing objects. In Table 3, our method consistently performs well across different editing types. Figure 5 illustrates qualitative examples of ALE-Edit for various editing types. These results indicate that our method can effectively manage attribute changes of various types without unintended alterations in non-targeted areas. Detailed settings and results are in Appendix D and E.

4.3. Ablation Studies

We also present ablation experiment results on RGB-CAM and BB in Figure 6. Using ORE alone successfully generates the target prompt (“diamond and moon”) but exhibits significant TI and TE leakage. Combining ORE with RGB-CAM reduces TI leakage but still suffers from TE leakage. Conversely, combining ORE with BB mitigates TE leakage but shows considerable TI leakage. Additional ablation results can be found in Appendix F.

5. Conclusion

In this paper, we addressed the issue of attribute leakage in diffusion-based image editing with our proposed framework, ALE-Edit. To minimize TI leakage, we proposed object-restricted embeddings (ORE) and region-guided blending for cross-attention masking (RGB-CAM) method. For TE leakage, we implemented background blending (BB) method that blends source latent for the background with target latent for the object.

We also introduced the Attribute Leakage Evaluation Benchmark (ALE-Bench), designed to rigorously assess attribute leakage across diverse editing scenarios. ALE-Bench includes new metrics—TI and TE Leakage—to accurately quantify unintended modifications.

Our experimental results demonstrate that combining ORE with RGB-CAM and BB significantly mitigates attribute leakage, enabling more precise and reliable image editing. By reducing dependency on complex prompts and delivering high-fidelity edits, our work advances the development of practical image editing applications.

References

- [1] Omri Avrahami, Rinon Gal, Gal Chechik, Ohad Fried, Dani Lischinski, Arash Vahdat, and Weili Nie. Diffuhaul: A training-free method for object dragging in images. *arXiv preprint arXiv:2406.01594*, 2024. 1
- [2] Tim Brooks, Aleksander Holynski, and Alexei A Efros. Instructpix2pix: Learning to follow image editing instructions. In *Proceedings of the IEEE/CVF Conference on Computer Vision and Pattern Recognition*, pages 18392–18402, 2023. 1
- [3] Mingdeng Cao, Xintao Wang, Zhongang Qi, Ying Shan, Xiaohu Qie, and Yinqiang Zheng. Masactrl: Tuning-free mutual self-attention control for consistent image synthesis and editing. In *Proceedings of the IEEE/CVF International Conference on Computer Vision*, pages 22560–22570, 2023. 1, 3
- [4] Goirik Chakrabarty, Aditya Chandrasekar, Ramya Hebbalaguppe, and Prathosh AP. Lomoe: Localized multi-object editing via multi-diffusion. In *Proceedings of the 32nd ACM International Conference on Multimedia*, pages 3342–3351, 2024. 2
- [5] Jooyoung Choi, Sungwon Kim, Yonghyun Jeong, Youngjune Gwon, and Sungroh Yoon. Ilvr: Conditioning method for denoising diffusion probabilistic models. *arXiv preprint arXiv:2108.02938*, 2021. 1
- [6] Prafulla Dhariwal and Alexander Nichol. Diffusion models beat gans on image synthesis. *Advances in neural information processing systems*, 34:8780–8794, 2021. 1
- [7] Adham Elarabawy, Harish Kamath, and Samuel Denton. Direct inversion: Optimization-free text-driven real image editing with diffusion models. *arXiv preprint arXiv:2211.07825*, 2022. 1, 6
- [8] Weixi Feng, Xuehai He, Tsu-Jui Fu, Varun Jampani, Arjun Akula, Pradyumna Narayana, Sugato Basu, Xin Eric Wang, and William Yang Wang. Training-free structured diffusion guidance for compositional text-to-image synthesis. *arXiv preprint arXiv:2212.05032*, 2022. 1, 4
- [9] Qin Guo and Tianwei Lin. Focus on your instruction: Fine-grained and multi-instruction image editing by attention modulation. In *Proceedings of the IEEE/CVF Conference on Computer Vision and Pattern Recognition*, pages 6986–6996, 2024. 1
- [10] Ligong Han, Yinxiao Li, Han Zhang, Peyman Milanfar, Dimitris Metaxas, and Feng Yang. Svdif: Compact parameter space for diffusion fine-tuning. In *Proceedings of the IEEE/CVF International Conference on Computer Vision*, pages 7323–7334, 2023. 1
- [11] Amir Hertz, Ron Mokady, Jay Tenenbaum, Kfir Aberman, Yael Pritch, and Daniel Cohen-Or. Prompt-to-prompt image editing with cross attention control. *arXiv preprint arXiv:2208.01626*, 2022. 2, 3, 6, 1
- [12] Jonathan Ho and Tim Salimans. Classifier-free diffusion guidance. *arXiv preprint arXiv:2207.12598*, 2022. 1
- [13] Jonathan Ho, Ajay Jain, and Pieter Abbeel. Denoising diffusion probabilistic models. *Advances in neural information processing systems*, 33:6840–6851, 2020. 1, 3
- [14] Mingzhen Huang, Jialing Cai, Shan Jia, Vishnu Suresh Lokhande, and Siwei Lyu. Paralleledits: Efficient multi-aspect text-driven image editing with attention grouping. In *The Thirty-eighth Annual Conference on Neural Information Processing Systems*, 2024. 1, 2
- [15] Wenjing Huang, Shikui Tu, and Lei Xu. Pfb-diff: Progressive feature blending diffusion for text-driven image editing. *Neural Networks*, 181:106777, 2025. 2
- [16] Bahjat Kawar, Michael Elad, Stefano Ermon, and Jiaming Song. Denoising diffusion restoration models. *Advances in Neural Information Processing Systems*, 35:23593–23606, 2022. 1
- [17] Sunwoo Kim, Wooseok Jang, Hyunsu Kim, Junho Kim, Yunje Choi, Seungryong Kim, and Gayeong Lee. User-friendly image editing with minimal text input: Leveraging captioning and injection techniques. *arXiv preprint arXiv:2306.02717*, 2023. 2
- [18] Alexander Kirillov, Eric Mintun, Nikhila Ravi, Hanzi Mao, Chloe Rolland, Laura Gustafson, Tete Xiao, Spencer Whitehead, Alexander C. Berg, Wan-Yen Lo, Piotr Dollár, and Ross Girshick. Segment anything. *arXiv:2304.02643*, 2023. 5, 1
- [19] Shanglin Li, Bohan Zeng, Yutang Feng, Sicheng Gao, Xiuhui Liu, Jiaming Liu, Lin Li, Xu Tang, Yao Hu, Jianzhuang Liu, et al. Zone: Zero-shot instruction-guided local editing. In *Proceedings of the IEEE/CVF Conference on Computer Vision and Pattern Recognition*, pages 6254–6263, 2024. 1, 2
- [20] Bingyan Liu, Chengyu Wang, Tingfeng Cao, Kui Jia, and Jun Huang. Towards understanding cross and self-attention in stable diffusion for text-guided image editing. In *Proceedings of the IEEE/CVF Conference on Computer Vision and Pattern Recognition*, pages 7817–7826, 2024. 1, 3
- [21] Mushui Liu, Yuhang Ma, Yang Zhen, Jun Dan, Yunlong Yu, Zeng Zhao, Zhipeng Hu, Bai Liu, and Changjie Fan. Llm4gen: Leveraging semantic representation of llms for text-to-image generation. *arXiv preprint arXiv:2407.00737*, 2024. 2
- [22] Minghao Liu, Le Zhang, Yingjie Tian, Xiaochao Qu, Luoqi Liu, and Ting Liu. Draw like an artist: Complex scene generation with diffusion model via composition, painting, and retouching. *arXiv preprint arXiv:2408.13858*, 2024. 2, 1
- [23] Shilong Liu, Zhaoyang Zeng, Tianhe Ren, Feng Li, Hao Zhang, Jie Yang, Chunyuan Li, Jianwei Yang, Hang Su, Jun Zhu, et al. Grounding dino: Marrying dino with grounded pre-training for open-set object detection. *arXiv preprint arXiv:2303.05499*, 2023. 5, 1
- [24] Simian Luo, Yiqin Tan, Longbo Huang, Jian Li, and Hang Zhao. Latent consistency models: Synthesizing high-resolution images with few-step inference. *arXiv preprint arXiv:2310.04378*, 2023. 3
- [25] Zhiyuan Ma, Guoli Jia, and Bowen Zhou. Adapedit: Spatio-temporal guided adaptive editing algorithm for text-based continuity-sensitive image editing. In *Proceedings of the AAAI Conference on Artificial Intelligence*, pages 4154–4161, 2024. 2
- [26] Qi Mao, Lan Chen, Yuchao Gu, Zhen Fang, and Mike Zheng Shou. Mag-edit: Localized image editing in complex sce-

- narios via mask-based attention-adjusted guidance. *arXiv preprint arXiv:2312.11396*, 2023. 2, 1
- [27] Chenlin Meng, Yutong He, Yang Song, Jiaming Song, Jiajun Wu, Jun-Yan Zhu, and Stefano Ermon. Sdedit: Guided image synthesis and editing with stochastic differential equations. *arXiv preprint arXiv:2108.01073*, 2021. 1
- [28] Ron Mokady, Amir Hertz, Kfir Aberman, Yael Pritch, and Daniel Cohen-Or. Null-text inversion for editing real images using guided diffusion models. In *Proceedings of the IEEE/CVF Conference on Computer Vision and Pattern Recognition*, pages 6038–6047, 2023. 1, 3
- [29] Trong-Tung Nguyen, Duc-Anh Nguyen, Anh Tran, and Cuong Pham. Flexedit: Flexible and controllable diffusion-based object-centric image editing. *arXiv preprint arXiv:2403.18605*, 2024. 2
- [30] Alex Nichol, Prafulla Dhariwal, Aditya Ramesh, Pranav Shyam, Pamela Mishkin, Bob McGrew, Ilya Sutskever, and Mark Chen. Glide: Towards photorealistic image generation and editing with text-guided diffusion models. *arXiv preprint arXiv:2112.10741*, 2021. 1
- [31] Gaurav Parmar, Krishna Kumar Singh, Richard Zhang, Yijun Li, Jingwan Lu, and Jun-Yan Zhu. Zero-shot image-to-image translation. In *ACM SIGGRAPH 2023 Conference Proceedings*, pages 1–11, 2023. 2, 1
- [32] Dustin Podell, Zion English, Kyle Lacey, Andreas Blattmann, Tim Dockhorn, Jonas Müller, Joe Penna, and Robin Rombach. Sdxl: Improving latent diffusion models for high-resolution image synthesis. *arXiv preprint arXiv:2307.01952*, 2023. 1
- [33] Alec Radford, Jong Wook Kim, Chris Hallacy, Aditya Ramesh, Gabriel Goh, Sandhini Agarwal, Girish Sastry, Amanda Askell, Pamela Mishkin, Jack Clark, et al. Learning transferable visual models from natural language supervision. In *International conference on machine learning*, pages 8748–8763. PMLR, 2021. 1
- [34] Tianhe Ren, Shilong Liu, Ailing Zeng, Jing Lin, Kunchang Li, He Cao, Jiayu Chen, Xinyu Huang, Yukang Chen, Feng Yan, Zhaoyang Zeng, Hao Zhang, Feng Li, Jie Yang, Hongyang Li, Qing Jiang, and Lei Zhang. Grounded sam: Assembling open-world models for diverse visual tasks, 2024. 5, 1
- [35] Robin Rombach, Andreas Blattmann, Dominik Lorenz, Patrick Esser, and Björn Ommer. High-resolution image synthesis with latent diffusion models. In *Proceedings of the IEEE/CVF conference on computer vision and pattern recognition*, pages 10684–10695, 2022. 1
- [36] Nataniel Ruiz, Yuanzhen Li, Varun Jampani, Yael Pritch, Michael Rubinstein, and Kfir Aberman. Dreambooth: Fine tuning text-to-image diffusion models for subject-driven generation. In *Proceedings of the IEEE/CVF conference on computer vision and pattern recognition*, pages 22500–22510, 2023. 1
- [37] Shelly Sheynin, Adam Polyak, Uriel Singer, Yuval Kirstain, Amit Zohar, Oron Ashual, Devi Parikh, and Yaniv Taigman. Emu edit: Precise image editing via recognition and generation tasks. In *Proceedings of the IEEE/CVF Conference on Computer Vision and Pattern Recognition*, pages 8871–8879, 2024. 1
- [38] Enis Simsar, Alessio Tonioni, Yongqin Xian, Thomas Hofmann, and Federico Tombari. Lime: Localized image editing via attention regularization in diffusion models. *arXiv preprint arXiv:2312.09256*, 2023. 2
- [39] Jascha Sohl-Dickstein, Eric Weiss, Niru Maheswaranathan, and Surya Ganguli. Deep unsupervised learning using nonequilibrium thermodynamics. In *International conference on machine learning*, pages 2256–2265. PMLR, 2015. 1
- [40] Jiaming Song, Chenlin Meng, and Stefano Ermon. Denoising diffusion implicit models. *arXiv preprint arXiv:2010.02502*, 2020. 1
- [41] Yang Song, Jascha Sohl-Dickstein, Diederik P Kingma, Abhishek Kumar, Stefano Ermon, and Ben Poole. Score-based generative modeling through stochastic differential equations. *arXiv preprint arXiv:2011.13456*, 2020. 1
- [42] Chuanming Tang, Kai Wang, Fei Yang, and Joost van de Weijer. Locinv: Localization-aware inversion for text-guided image editing. *arXiv preprint arXiv:2405.01496*, 2024. 1, 3
- [43] Maria Mihaela Trusca, Tinne Tuytelaars, and Marie-Francine Moens. Dm-align: Leveraging the power of natural language instructions to make changes to images. *arXiv preprint arXiv:2404.18020*, 2024. 1
- [44] Narek Tumanyan, Omer Bar-Tal, Shai Bagon, and Tali Dekel. Splicing vit features for semantic appearance transfer. In *Proceedings of the IEEE/CVF Conference on Computer Vision and Pattern Recognition*, pages 10748–10757, 2022. 7
- [45] Tsung-Han Wu, Long Lian, Joseph E Gonzalez, Boyi Li, and Trevor Darrell. Self-correcting llm-controlled diffusion models. In *Proceedings of the IEEE/CVF Conference on Computer Vision and Pattern Recognition*, pages 6327–6336, 2024. 1
- [46] Sihan Xu, Yidong Huang, Jiayi Pan, Ziqiao Ma, and Joyce Chai. Inversion-free image editing with natural language. *arXiv preprint arXiv:2312.04965*, 2023. 1, 3, 6, 7, 2, 4
- [47] Fei Yang, Shiqi Yang, Muhammad Atif Butt, Joost van de Weijer, et al. Dynamic prompt learning: Addressing cross-attention leakage for text-based image editing. *Advances in Neural Information Processing Systems*, 36:26291–26303, 2023. 1, 2, 3
- [48] Ling Yang, Zhaochen Yu, Chenlin Meng, Minkai Xu, Stefano Ermon, and CUI Bin. Mastering text-to-image diffusion: Recaptioning, planning, and generating with multimodal llms. In *Forty-first International Conference on Machine Learning*, 2024. 1, 4
- [49] Yi Yao, Chan-Feng Hsu, Jhe-Hao Lin, Hongxia Xie, Terence Lin, Yi-Ning Huang, Hong-Han Shuai, and Wen-Huang Cheng. The fabrication of reality and fantasy: Scene generation with llm-assisted prompt interpretation. In *European Conference on Computer Vision*, pages 422–438. Springer, 2025. 1
- [50] Lvmin Zhang, Anyi Rao, and Maneesh Agrawala. Adding conditional control to text-to-image diffusion models. In *Proceedings of the IEEE/CVF International Conference on Computer Vision*, pages 3836–3847, 2023. 1
- [51] Yang Zhang, Rui Zhang, Xuecheng Nie, Haochen Li, Jikun Chen, Yifan Hao, Xin Zhang, Luoqi Liu, and Ling Li.

Spdiffusion: Semantic protection diffusion for multi-concept text-to-image generation. *arXiv preprint arXiv:2409.01327*, 2024. [1](#), [2](#), [4](#)

- [52] Siyu Zou, Jiji Tang, Yiyi Zhou, Jing He, Chaoyi Zhao, Rongsheng Zhang, Zhipeng Hu, and Xiaoshuai Sun. Towards efficient diffusion-based image editing with instant attention masks. In *Proceedings of the AAAI Conference on Artificial Intelligence*, pages 7864–7872, 2024. [1](#), [2](#)

Addressing Attribute Leakages in Diffusion-based Image Editing without Training

Supplementary Material

A. Related Work

A.1. Text-to-Image Diffusion Models

As a class of generative models, Diffusion models [6, 13, 39–41] have gained a reputation with their performance. Furthermore, classifier-free diffusion guidance [12] proposed conditional generation of diffusion models and GLIDE [30] integrated CLIP text encoder [33] into diffusion models for text-to-image generation. Introducing the latent diffusion model that denoises a latent rather than an image, StableDiffusion [35] enlarged the potential of diffusion models by greatly reducing their computational complexity and publishing pre-trained multi-modal conditioning diffusion models. Even more, SDXL [32] trained a model aiming to generate an image with only a single step, optionally requiring multi-steps. Personalization of diffusion models [10, 36] is another line of work, where the goal is to generate a specific user-defined object. For planning and iterating the diffusion process, large language models are also used [22, 45, 48, 49] to understand user’s needs and confirm whether resulting images satisfy it.

A.2. Controllable Generation Process

Based on their outstanding performance of open-source pre-trained models, the user-controllable generation process is widely studied in the context of both tuning [50] and tuning-free [8, 12, 30]. ControlNet [50] provides a method to train a module that conditions pre-trained text-to-image diffusion models with arbitrary multi-modality, such as sketch, depth map, canny edges, human pose, or image. Instruct-Pix2Pix [2] is an image editing model that fine-tuned StableDiffusion [35], generating an edited image instructed with natural language, e.g. “Swap sunflowers with roses”, “Add Fireworks to the sky”. Instead of tuning a model, several methods [31] optimized a parameter and froze the model parameter.

However, because of their heavy computational complexity, tuning-based methods are not transferable to models that differ from the model to which they are applied. Without requiring additional resources, tuning-free methods control the generation process by conditioning on initial noise [27], attention layers [3, 8, 11, 51], or using a third-party module [48], such as LLM or GroundedSAM [18, 23, 34].

A.3. Image Editing

Branching from image generation, image editing aims its unique goals, refer to Section 2.2 for details. It can be divided into two categories (1) training a model or optimizing parameters [2, 26, 28, 37, 47] and (2) tuning-free approaches [3, 11, 43, 46, 52]. The latter is related to our work, where self-attention layer control [52] and Virtual Inversion [46] are directly applied to our framework. Prompt-to-Prompt (P2P) [11] edits an image by injecting cross-attention values which contain its structural information. MasaCtrl [3] and Free-Prompt-Editing (FPE) [52] instead inject self-attention values, where MasaCtrl changes key K and value V , and FPE changes query Q and key K of target image into those of source. Additional hyperparameters are required for both methods, specifying (1) from which layer and (2) from which timesteps to inject self-attention values, where the second is called a self-attention control schedule.

Another group of study focuses on that, though diffusion models show their remarkable performance, perfect reconstruction of arbitrary image still remains as a hard problem for both artificial (generated by a model) and natural (taken in a real world) images. With an intuition that the better reconstruction yields the better resource for editing, this line of works studies how to perform better inversion in a tuning-based [28, 47] and a tuning-free [46] manner. Null Text Inversion [28] and Dynamic Prompt Learning [47] optimize a null text prompt, where DPL focuses on attribute leakage with self-attention maps clustering and a proposed loss. However, their optimizing processes require 2 to 4 minutes for a single image editing, limiting their applicability on a large dataset. InfEdit [46] introduces Virtual Inversion, in the sense that the inversion process can utilize both a clean source image and a degraded image generated by a diffusion model through the denoising process.

B. Benchmark Construction Details

Benchmark overview Our benchmark is designed to evaluate attribute leakage in image editing tasks using diffusion models. Unlike existing benchmarks that focus on image quality and background preservation, our benchmark emphasizes preventing unintended changes in both target-external and target-internal regions. It consists of 20 diverse images, semi-automated object masks, and succinct prompt pairs for various editing types. To comprehensively evaluate models, we generate 10 random edit prompts for each combination of 5 edit types and 1–3 edited objects per im-




Source Image	Color	Object	Material	Color+ Object	Object+ Material
	yoga mat → pink-colored yoga mat	man → alien	footwear → footwear made of amber	footwear → orange-colored sandals	man → woman made of bronze
	cup → white-colored cup, steam → green-colored steam	book → cushion, cup → tumbler	book → book made of chrome, cup → cup made of paper	steam → gray-colored smoke, cup → blue-colored jar	book → journal made of gold, cup → mug made of amethyst
	wolf → pink-colored wolf, moon → purple-colored moon, mountain → gray-colored mountain	wolf → eagle, moon → soccer ball, mountain → glacier	wolf → wolf made of velvet, moon → moon made of steel, mountain → mountain made of leather	wolf → crimson-colored dragon, moon → navy-colored soccer ball, mountain → brown-colored garden	wolf → dog made of linen, moon → balloon made of paper, mountain → glacier made of amber

Figure 7. Examples from ALE-Bench. Source object masks are overlaid on source images. Edit types are color, object, material modifications, and their combinations. The first row shows single-object edits, the second row showcases two-object edits, and the third row illustrates three-object edits.

age, resulting in a total of 3,000 diverse editing scenarios. To quantify attribute leakage, we introduce novel metrics: Target-External Leakage (TE) and Target-Internal Leakage (TI). By covering diverse editing scenarios and offering precise evaluation metrics, our benchmark provides a robust framework for improving the precision of image editing methods. Figure 7 illustrates examples, showing the source images, object masks, and associated editing prompts.

Image selection We curated a dataset of 20 images, evenly split between natural and artificial scenes, to provide diverse and challenging editing scenarios. All images were drawn from both free image repositories and the PIE-bench dataset [46]. To ensure complexity, we included only images containing at least three distinct objects.

Prompt construction ALE-Bench provides five editing types. The prompt templates for different editing types are as follows:

1. Color change: “{color}-colored {object}” (e.g., “car” → “red-colored car”).
2. Object change: “{new object}” (e.g., “car” → “bus”).
3. Material change: “{object} made of {material}” (e.g., “car” → “car made of gold”).
4. Color and object change: “{color}-colored {new object}” (e.g., “car” → “blue-colored bus”).

5. Object and material change: “{new object} made of {material}” (e.g., “car” → “bus made of gold”).

We intentionally excluded combinations like “color and material” and “color, object and material” because such cases often lead to unrealistic or ambiguous prompts, such as “silver-colored car made of gold”. These kinds of descriptions are inherently challenging to interpret or generate, even for a human, making them impractical editing scenarios.

For each image, we generated 10 unique and random edit prompt instances for every combination of edit type and number of objects to edit. These prompts were created using attribute dictionaries containing target instances for colors, objects, and materials, with the assistance of ChatGPT to ensure diversity and consistency. This approach results in a systematic exploration of the attribute space across 20 images, 5 edit types, and varying numbers of objects, covering a total of 3,000 unique editing scenarios. Additionally, we emphasize the importance of user convenience by designing minimal prompt pairs that specify only the intended modification, avoiding the verbosity commonly seen in previous benchmarks.

Evaluation metrics In addition to standard metrics from PIE-bench—such as structural distance, background preservation (PSNR, SSIM, LPIPS, MSE), and editing perfor-

mance (CLIP similarity)—we propose two novel metrics specifically designed to evaluate attribute leakage. The Target-External (TE) Leakage metric quantifies unintended changes to background regions during editing. This is calculated by measuring the CLIP scores between the background regions of the edited image and the target prompt (Equation 6). Lower TE leakage values indicate minimal impact on the background, ensuring that non-edited regions remain unaffected. The Target-Internal (TI) Leakage metric captures unintended cross-influence between multiple edited objects. For each edited object, we compute the CLIP scores between its edited region and the prompts intended for other objects, then take the mean scores across all object pairs (Equation 5). Lower TI leakage values indicate that edits are confined to their respective objects without unintended interactions or overlaps.

C. Notation Details

Text embeddings are denoted as $e \in \mathbb{R}^{N \times D}$, where N is the maximum number of tokens and D is the embedding dimension. We used $N = 77$ and $D = 768$ in all experiments. For object O_i represented by multiple L tokens, $e[O_i] \in \mathbb{R}^{L \times D}$ refers to the embeddings of all tokens associated with O_i .

Object masks are represented as $mask \in \{0, 1\}^{W \times H}$, where W and H are the width and height of the image. m_i denotes the mask of the i -th object obtained by GroundedSAM. Since a target prompt corresponds to multiple tokens, the function `associate_masks` in Algorithm 2 associates the corresponding masks to the target prompt tokens to create $m_list \in \{0, 1\}^{N \times W \times H}$ array.

D. Experiments Details

Common settings All methods were evaluated using the Latent Consistency Model (LCM) to ensure consistency across all experiments [24]. The generation resolution for all images was set to 768×768 , maintaining high quality and comparability across results. All experiments were conducted on a single NVIDIA RTX A6000 or RTX 6000 Ada Generation GPU.

Prompt construction For methods such as MasaCtrl and FPE that require only a single target prompt, the target prompt was constructed by concatenating all target object prompts with “and” to form a prompt. For methods like P2P and InfEdit that require both a source and a target prompt, the source prompt was similarly created by concatenating the source object prompts, while the target prompt was constructed by concatenating the target object prompts.

Hyperparameters For our method, we set the inference steps to 15 and the mask dilation ratio to 0.01, correspond-

ing to a dilation of seven pixels. The self-attention control schedule was adjusted according to the type of edit: 1.0 for colors, 0.5 for objects, color+object, and material+object, and 0.6 for material. The same self-attention control schedule was applied to InfEdit and P2P, as this hyperparameter is shared. For all other hyperparameters of the baseline methods (MasaCtrl, FPE, P2P, InfEdit), we used the default settings provided in their official implementations.

E. Additional Results

By object count Tables 4, 5, and 6 present the quantitative evaluation of our method and baselines on ALE-Bench across different numbers of editing objects. For the baseline methods, TE and TI leakage values decrease as the number of edited objects increases, as editing more objects provides a more detailed description of the image, reducing ambiguity. This trend highlights the baselines’ dependence on long and detailed prompts. However, their editing performance decreases with an increasing number of edited objects, revealing their limitations in handling complex edits. In contrast, our method demonstrates robust performance across all object counts, consistently achieving the lowest leakage values, preserving structure and background, and maintaining competitive or superior editing performance.

By edit type We compare our methods with baselines across different edit types in Tables 7, 8, 9, 10, and 11. Across all edit types, our method consistently outperforms baselines by achieving lower leakage, better structural and background preservation, and strong editing performance. We provide more qualitative examples on ALE-Bench for each edit type in two objects editing in Figure 8.

F. Ablation Study Results

Ablation on EOS embedding methods To evaluate the effect of EOS embeddings, we studied several methods of modifying EOS embeddings: (1) Naïve: No modification, using the original EOS embeddings; (2) Zeros: Replacing EOS embeddings with zero-valued vectors; (3) BOS: Substituting EOS embeddings with BOS (beginning-of-sequence) embeddings; (4) Empty String: Using EOS embeddings derived from an empty string. In Figure 6, our method demonstrates robust results across various scenarios, while the other methods often produce images that fail to follow the edit prompt or exhibit attribute leakage. A detailed quantitative comparison is provided in Table 12.

Our method consistently achieves the best editing performance while maintaining competitive structure and background preservation metrics. In contrast, the other methods reveal a trade-off between reducing leakage and maintaining high editing performance, highlighting the effectiveness of our approach in balancing these objectives.

Ablation on RGB-CAM and BB The results in Table 13 demonstrate the complementary strengths of RGB-CAM and BB in our method. While RGB-CAM effectively reduces TI leakage by confining edits to the targeted objects, its impact on TE leakage and background preservation is limited. Conversely, BB significantly lowers TE leakage by preserving non-edited regions, improving background quality but slightly reducing editing performance. Combining all components (Ours) achieves the best overall balance, minimizing leakage while preserving structure and background, and maintaining strong editing performance, highlighting the synergy of these components.

Evaluation on PIE-Bench We also evaluated our method on the existing PIE-Bench [46] in addition to ALE-Bench. Since our method does not support all edit types in PIE-Bench, we conducted experiments on the four edit types that are compatible: *object change*, *content change*, *color change*, and *material change*.

PIE-Bench only considers scenarios with a single editing object, so we excluded the TI Leakage metric. When running our method, we used the blend word provided by PIE-Bench as the SAM prompt for mask generation. In cases where mask segmentation failed, we edited the image without cross-attention masking and background blending.

In Table 14, the results show that our method demonstrated the lowest attribute leakage and high editing performance among all methods, even on PIE-Bench. These findings further validate the robustness and versatility of our approach across different benchmarks. We also provide qualitative examples for each edit type from the PIE-Bench experiments in Figure 10.

Ablation on self-attention schedule The degree to which the structure of a source image needs to be preserved varies depending on the edit type. For edits like color changes, maintaining the original structure is crucial, while object changes may require more deviation from the source. Figure 6 shows the effect of the self-attention schedule across various scenarios. Adjusting the schedule from 0.0 to 1.0 shows that higher values preserve more structure, while lower values allow greater flexibility. Thus, selecting the appropriate self-attention schedule depends on the specific goals of the task. The hyperparameters we used, detailed in Appendix D, were chosen based on these experimental findings.

G. Limitations

ALE-Bench While our benchmark offers a robust framework for evaluating attribute leakage, it has limitations. It focuses on basic and mixed edits (e.g., color, object, material changes) and does not cover more complex tasks like

style transfer or add/delete objects, where defining attribute leakage is ambiguous. Additionally, the dataset size (20 images) may limit evaluations of models trained on larger or more diverse datasets. Future works could address these limitations by expanding the dataset and incorporating more diverse editing tasks.



Figure 12. Failure case due to the base model’s inability. Editing prompt: *cloud* → cloud made of **chrome**. Figure 12c illustrates the generation result when given the prompt “cloud made of chrome”.



Figure 13. Failure case due to SAM segmentation fail. Editing prompt: *... cat ...* → *... panda ...*. Figure 13c shows the unsuccessful segmentation of SAM.

Failure cases Our framework leverages two backbone models, a pre-trained diffusion model and a segmentation model, Grounded-SAM. Consequently, it may fail when the task exceeds the capabilities of these backbone models. For instance, overly rare or complex prompts that the pre-trained diffusion model cannot handle (Figure 12), objects that are difficult for the segmentation model to recognize, or incomplete segmentation masks generated by the model (Figure 13) can lead to unsatisfactory results. However, since our method operates in parallel with advancements in these backbone models, we anticipate that such failure cases will decrease as these models continue to improve.

Method	TE Leakage	TI leakage	Structure Preservation	Editing Performance	Background Preservation			
	CS ↓	CS ↓	SD ↓	Edited ↑	PSNR ↑	LPIPS ↓	MSE ↓	SSIM ↑
P2P	24.88	NaN	0.1526	21.49	10.29	0.5302	0.10330	0.4752
MasaCtrl	23.32	NaN	0.1009	20.47	13.73	0.3681	0.05269	0.6636
FPE	24.43	NaN	0.1195	22.85	11.63	0.4691	0.08074	0.5159
InfEdit	21.97	NaN	0.0506	22.62	15.31	0.2509	0.04397	0.7049
Ours	16.21	NaN	0.0089	22.54	30.13	0.0394	0.00134	0.9046

Table 4. Quantitative evaluation of **editing one object** for our method and baselines on ALE-Bench.

Method	TE Leakage	TI leakage	Structure Preservation	Editing Performance	Background Preservation			
	CS ↓	CS ↓	SD ↓	Edited ↑	PSNR ↑	LPIPS ↓	MSE ↓	SSIM ↑
P2P	20.81	17.45	0.1515	20.35	11.09	0.4496	0.08775	0.5554
MasaCtrl	19.52	16.78	0.0913	19.81	14.95	0.2904	0.04115	0.7337
FPE	20.42	17.58	0.1166	21.61	12.77	0.3885	0.06516	0.6020
InfEdit	19.15	16.75	0.0488	21.40	16.64	0.2042	0.03330	0.7709
Ours	15.97	15.31	0.0166	21.97	30.04	0.0362	0.00139	0.9223

Table 5. Quantitative evaluation of **editing two objects** for our method and baselines on ALE-Bench.

Method	TE Leakage	TI leakage	Structure Preservation	Editing Performance	Background Preservation			
	CS ↓	CS ↓	SD ↓	Edited ↑	PSNR ↑	LPIPS ↓	MSE ↓	SSIM ↑
P2P	18.74	16.94	0.1547	20.00	12.01	0.3681	0.07440	0.6444
MasaCtrl	17.53	16.46	0.0868	19.41	16.21	0.2253	0.03314	0.8014
FPE	18.35	16.98	0.1187	20.88	13.97	0.3159	0.05295	0.6881
InfEdit	17.63	16.43	0.0466	21.02	18.12	0.1596	0.02579	0.8343
Ours	15.91	15.26	0.0246	22.09	29.94	0.0328	0.00158	0.9414

Table 6. Quantitative evaluation of **editing three objects** for our method and baselines on ALE-Bench.

Method	TE Leakage	TI leakage	Structure Preservation	Editing Performance	Background Preservation			
	CS ↓	CS ↓	SD ↓	Edited ↑	PSNR ↑	LPIPS ↓	MSE ↓	SSIM ↑
P2P	23.07	17.91	0.1479	21.86	10.98	0.4536	0.0916	0.5719
MasaCtrl	21.48	17.07	0.0963	21.34	14.53	0.3148	0.0467	0.7232
FPE	22.38	17.68	0.1077	22.97	12.57	0.3947	0.0709	0.6174
InfEdit	19.71	17.04	0.0351	22.88	18.39	0.1441	0.0283	0.8316
Ours	17.66	15.93	0.0091	22.85	32.89	0.0294	0.0008	0.9293

Table 7. Quantitative evaluation of the **color change** edit type for our method and baselines on ALE-Bench.

Method	TE Leakage	TI leakage	Structure Preservation	Editing Performance	Background Preservation			
	CS ↓	CS ↓	SD ↓	Edited ↑	PSNR ↑	LPIPS ↓	MSE ↓	SSIM ↑
P2P	20.59	17.74	0.1550	20.38	11.24	0.4447	0.0871	0.5499
MasaCtrl	19.52	17.33	0.0901	19.72	15.48	0.2744	0.0380	0.7417
FPE	19.75	17.57	0.1236	21.30	13.12	0.3735	0.0624	0.6097
InfEdit	18.67	17.13	0.0504	21.09	16.59	0.2118	0.0338	0.7605
Ours	15.80	16.28	0.0199	21.81	29.07	0.0382	0.0017	0.9212

Table 8. Quantitative evaluation of the **object change** edit type for our method and baselines on ALE-Bench.

Method	TE Leakage	TI leakage	Structure Preservation	Editing Performance	Background Preservation			
	CS ↓	CS ↓	SD ↓	Edited ↑	PSNR ↑	LPIPS ↓	MSE ↓	SSIM ↑
P2P	21.30	16.92	0.1552	20.59	11.04	0.4420	0.0877	0.5411
MasaCtrl	20.74	16.69	0.0870	20.67	15.30	0.28	0.0389	0.7385
FPE	21.83	17.42	0.1187	22.41	13.07	0.3800	0.0603	0.5893
InfEdit	20.26	16.65	0.0388	22.39	17.65	0.1765	0.0259	0.7852
Ours	17.09	15.71	0.0120	22.78	30.58	0.0344	0.0012	0.9235

Table 9. Quantitative evaluation of the **material change** edit type for our method and baselines on ALE-Bench.

Method	TE Leakage	TI leakage	Structure Preservation	Editing Performance	Background Preservation			
	CS ↓	CS ↓	SD ↓	Edited ↑	PSNR ↑	LPIPS ↓	MSE ↓	SSIM ↑
P2P	21.63	17.09	0.1504	20.72	11.11	0.4581	0.0899	0.5787
MasaCtrl	19.59	16.15	0.0986	19.18	14.43	0.3142	0.0463	0.7281
FPE	20.81	17.10	0.1165	21.39	12.42	0.4078	0.0718	0.6077
InfEdit	19.94	16.13	0.0620	21.26	15.02	0.2555	0.0453	0.7334
Ours	15.15	14.00	0.0228	22.14	28.70	0.0399	0.0018	0.9204

Table 10. Quantitative evaluation of the **color and object change** edit type for our method and baselines on ALE-Bench.

Method	TE Leakage	TI leakage	Structure Preservation	Editing Performance	Background Preservation			
	CS ↓	CS ↓	SD ↓	Edited ↑	PSNR ↑	LPIPS ↓	MSE ↓	SSIM ↑
P2P	20.80	16.30	0.1562	19.52	11.27	0.4483	0.0862	0.5500
MasaCtrl	19.28	15.86	0.0929	18.57	15.07	0.2893	0.0417	0.7332
FPE	20.56	16.63	0.1248	20.84	12.77	0.3998	0.0661	0.5860
InfEdit	19.34	16.01	0.0570	20.78	15.80	0.2367	0.0385	0.7395
Ours	14.47	14.49	0.0197	21.42	28.94	0.0387	0.0017	0.9195

Table 11. Quantitative evaluation of the **object and material change** edit type for our method and baselines on ALE-Bench.

Methods	TE Leakage	TI leakage	Structure Preservation	Editing Performance	Background Preservation			
	CS ↓	CS ↓	SD ↓	Edited ↑	PSNR ↑	LPIPS ↓	MSE ↓	SSIM ↑
Naïve	16.02	15.81	0.0156	21.86	30.14	0.0359	0.0014	0.9232
Zeros	15.74	15.23	0.0107	20.78	31.22	0.0327	0.0011	0.9254
BOS	15.76	15.27	0.0115	20.87	31.09	0.0334	0.0011	0.9241
Empty String	15.86	15.33	0.0139	21.25	30.61	0.0342	0.0013	0.9248
Ours	16.03	15.28	0.0167	22.20	30.04	0.0361	0.0014	0.9228

Table 12. Ablation study on different strategies for handling EOS embeddings in the prompt. While our method shows slightly higher leakages compared to others, it achieves the best editing performance. All experiments were conducted with both RGB-CAM and BB applied.



Figure 8. Qualitative examples of editing results for each edit type on ALE-Bench. Two examples are provided for each type. The left side of → represents the *source prompt*, and the right side represents the **target** prompt.

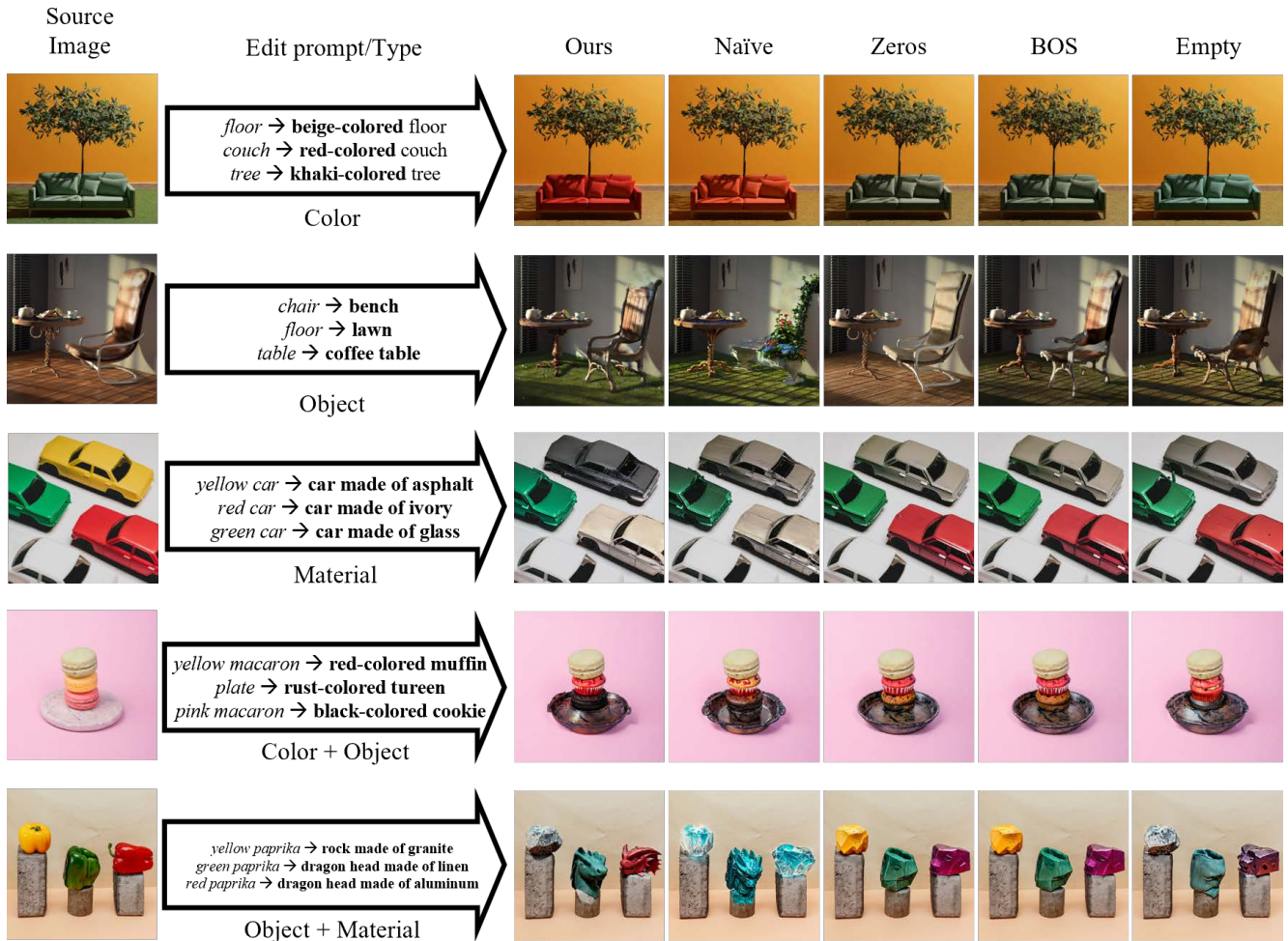


Figure 9. Qualitative examples from the EOS ablation study. While our method produces convincing results, other methods fail to generate the target object or exhibit attribute leakage. For instance, using the naive EOS to edit an object generates plants in place of the chair. This occurs due to attribute leakage from the word **lawn** to **bench**, resulting in chair-shaped flowers.

Methods	TE Leakage	TI leakage	Structure Preservation	Editing Performance	Background Preservation			
	CS ↓	CS ↓	SD ↓	Edited ↑	PSNR ↑	LPIPS ↓	MSE ↓	SSIM ↑
ORE	20.05	16.87	0.0521	21.81	16.16	0.2182	0.0380	0.7591
ORE+RGB	18.99	15.46	0.0436	22.42	17.48	0.1805	0.0291	0.7887
ORE+BB	16.12	16.58	0.0164	21.56	29.88	0.0368	0.0015	0.9219
Ours	16.03	15.28	0.0167	22.20	30.04	0.0361	0.0014	0.9228

Table 13. Ablation study results comparing different components of our method: object-restricted embeddings (ORE), region-guided blending cross-attention masking (RGB), and background blending (BB). RGB effectively reduces TI Leakage, while BB significantly lowers TE Leakage. Combining all components (ours) achieves the best overall performance across most metrics, demonstrating the synergy of integrating our methods.

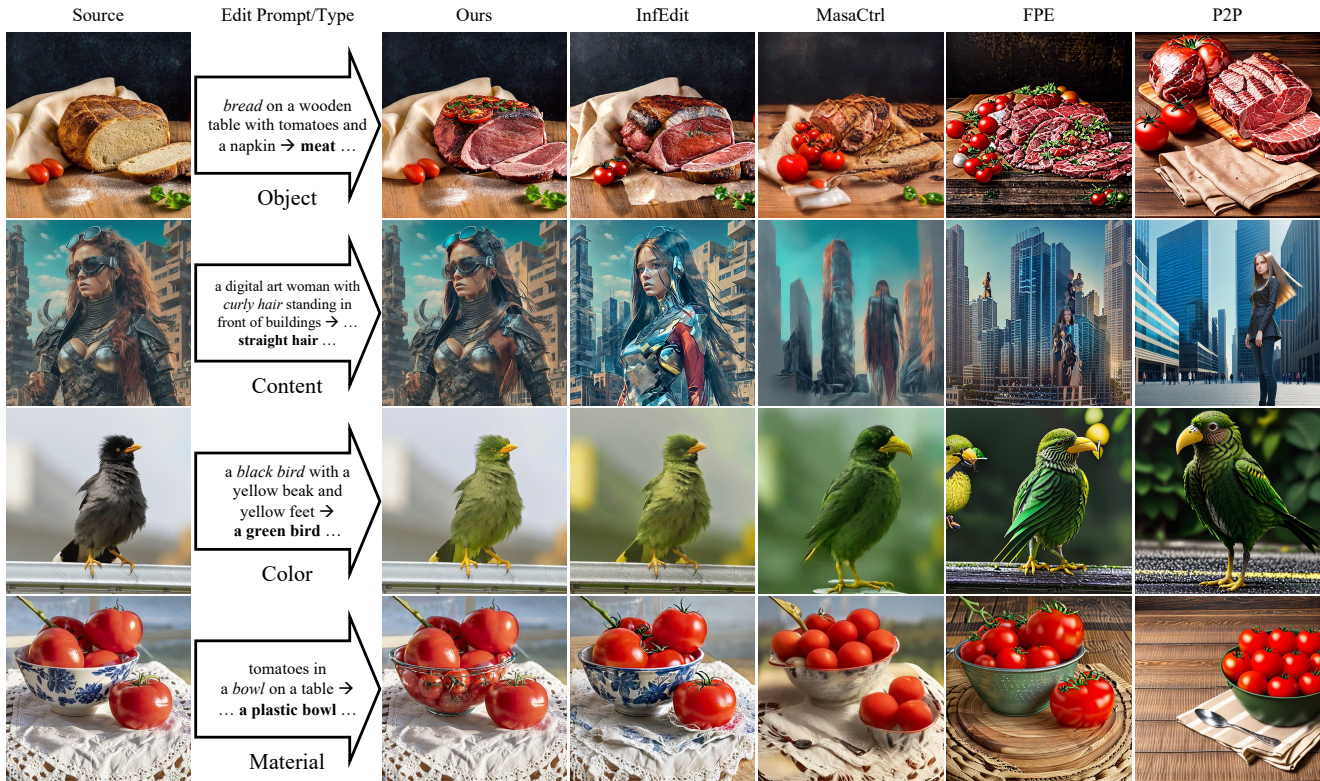


Figure 10. Qualitative examples of editing results for the four compatible edit types on PIE-Bench: object change, content change, color change, and material change. In edit prompt column, the left side of the arrow \rightarrow represents the source prompt, and the right side represents the target prompt, with unchanged parts omitted as “...” for brevity. The edited part is highlighted in *italic* and **bold**. Baseline methods exhibit attribute leakage or fail to preserve the source image structure, while our method achieves more precise edits with minimal leakage.

Method	TE Leakage	Structure Preservation	Editing Performance	Background Preservation			
	CS \downarrow	SD \downarrow	Edited \uparrow	PSNR \uparrow	LPIPS \downarrow	MSE \downarrow	SSIM \uparrow
P2P	26.20	0.1571	23.74	11.11	0.4270	0.0919	0.4600
MasaCtrl	24.48	0.0856	22.16	15.81	0.2540	0.0334	0.6803
FPE	25.64	0.1265	23.89	13.35	0.3499	0.0581	0.5346
InfEdit	24.51	0.0446	22.92	19.41	0.1519	0.0168	0.7581
Ours	22.94	0.0238	22.87	28.77	0.0580	0.0046	0.8865

Table 14. Evaluation results on PIE-Bench for compatible edit types (object change, content change, color change, and material change). Our method achieves the lowest TE leakage and demonstrates the best structure and background preservation while maintaining competitive editing performance.

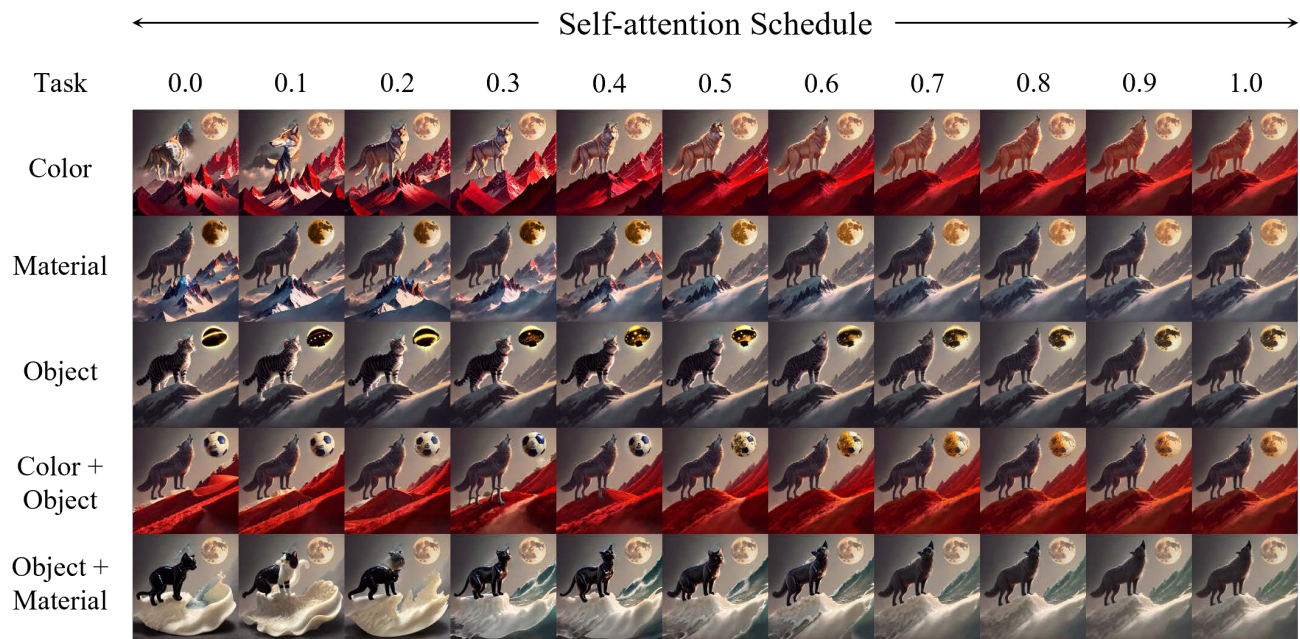


Figure 11. Ablation study on self-attention schedule, which controls when to inject self-attention layer values. For example, 0.3 represents that injection is performed during the first 30 percent of denoising timesteps. With higher schedule, more structure and content of the source image is preserved, and lower schedule gives more freedom. This trade-off requires different self-attention schedule across editing types. Followings are detailed prompts for each task; (1) color: *wolf* → **cream-colored** wolf, *mountain* → **crimson-colored** mountain, (2) material: *mountain* → mountain **made of crystal**, *moon* → moon **made of gold**, (3) object: *wolf* → **cat**, *moon* → **UFO**, (4) color + object: *moon* → **navy-colored soccer ball**, *mountain* → **crimson-colored hill**, (5) object + material: *cat* → wolf **made of rubber**, *mountain* → **wave made of ivory**